International Journal of Applied Engineering Research ISSN 0973-4562 Volume 14, Number 5 (2019) pp. 1126-1134

Enhancing Utilization of Solar Energy for the Application of Seawater Desalination

Amer Khalil Ababneh[1], Ali m. Jawarneh[2], Hitham Tlilan[2], Ahmad Migdadi[2]

[1] *Mechanical Engineering Department, Hashemite University. Currently, Spending Sabbatical at American University of Madaba, Madaba, Jordan.*

[2] *Mechanical Engineering Department, Hashemite University, Irbid-Mafrag hwy, Zarqa 13133 Jordan.*

Abstract

The article quantifies the improvement in performance of a solar-assisted scheme for the application of seawater desalination using parabolic trough collector by tilting the concentrators through small angles. Fossil fuel is used to augment the intermittence of solar irradiation. The scheme was analytically assessed under various solar conditions. Evaluation of performance included estimating the annual production of fresh water from seawater with the fuel only added to maintain a minimum daily production rate. The tilt angle improved the utilization of the incident solar radiation. For months with relatively low solar altitude angles; i.e., for March and October, it is revealed that with a tilt angle of 20° it resulted in improving the solar gain by 14% and 19%; respectively, while for months with high altitude angles the improvement was less. The improvement in solar gain has resulted in reducing the fuel heat requirement by about 44% for the month of October under certain conditions. Better utilization of solar energy has economical benefits as well as it leads to reducing the detrimental effects on the environment.

Keywords: utilization of solar energy, solar for desalination, tilting PTC, enhancing solar concentrator performance

Nomenclature

A_c	Aperture area of parabolic trough collector
C_n	Clearness Number
c_g	Glass specific heat capacitance
c_s	Steel specific heat capacitance
c_{wp}	Water specific heat at constant pressure
c_{wv}	Water specific heat at constant volume
dt	Incremental time change
dT_{wi}	Incremental temperature change for water in the ith node
dT_{si}	Incremental temperature change for steel in the ith node
dT_{gi}	Incremental temperature change for glass in the ith node
F_{amb}	Factor representing effect of environment condition on the collector such as dust. It is set at 0.94
h	Heat transfer coefficient inside the steel pipe, W/m^2-K
h_∞	Heat transfer coefficient for ambient air associated with glass outside, W/m^2-K
I_{b}	Solar direct beam intensity, W/m^2
k_s, k_g	Steel and glass thermal conductivity, W/m-K
K	Modifier factor that accounts for overall optical efficiency for angles other than normal.
$m\square_w$	Mass flow rate of water through the steel pipe
MED	Multiple-Effect Distillation
MSF	Multi-Stage Flash
Q_{cvi}	Heat convection from steel pipe inner walls to flowing water
Q_{gain}	The gained heat from the parabolic trough collector by the seawater
$Q_{\mathrm{gcv}\infty}$	Heat loss from glass to ambient through convection
$Q_{\mathrm{gr}\infty}$	The loss heat from the glass tube through radiation
Q_{si}	Solar energy incident on absorber after passing through glass tube
$Q_{\mathrm{sr}\infty}$	Heat loss from the steel pipe through radiation that passes through the glass tube
SEGS	Solar Electric Generating Stations
Q_{loss}	Heat loss from absorber through convection and radiation.
PTC	Parabolic Trough Collector
T_{gi}	Glass temperature of the ith node
T_{si}	Steel temperature of the ith node
T_{sur}	Surrounding temperature which is set equal to air temperature
T_{wi}	Water temperature of the ith node
T_∞	Ambient air temperature

Greek and mixed Symbols

δA_{go} Outside circumferential area of ith glass node

δA_{gc} Cross-sectional area of ith glass node

δA_{si} Inside circumferential area of ith steel node

δA_{sc} Cross-sectional area of the steel pipe

δA_{so} Outside circumferential area of ith steel node

δm_{wi} Water mass in the ith node

δm_{gi} Glass mass in the ith node

δm_{si} Steel mass in the ith node

ε_g, ε_s Glass and steel emissivity

ε_{slw} Portion of radiation emitted from steel directly to the outside

η_{norm} Peak optical efficiency at normal incidence; φ=0°.

φ Incidence angle; with angle 0° solar beam is normal to receiving horizontal plane.

σ Stephan-Boltzamn constant, $5.67\text{x}10^{-8}$ W/m^2-K^4

INTRODUCTION

Understandably the importance of energy for the various activities of mankind; however, equally important are the tapped resources for obtaining it since the limitation of fossil-fuel resources as well as their detrimental effects on the environment. This brings in the importance of renewable energy resources for complementing or supplying all the required energy. It is recognized among the range of available renewable energy resources that solar energy holds the most potential of all [1] for supplying required energy to various applications of which there is one that is essential and necessary for the continuation of life: it is seawater desalination. Also, it is repeatedly shown that using renewable resources is costly; therefore, improving their effectiveness is critical to their implementation.

The need for fresh water as a basic necessity for life is recognized by all individuals; however, according to [2] the world is facing water crisis and the problem will intensify unless effective measures are taken. It is becoming clear that seawater desalination is a plausible solution for sustaining supplies for future demands of fresh water, whereby this is evident from the growth of total contracted capacity for desalination which grew from near zero in 1965 to about 75 million m^3 of fresh water per day [3]. Seawater desalination is energy demanding, thus optimization and better utilization of renewable energy resources are heavily investigated for reducing the cost of the production of fresh water. To illustrate this it is estimated that for producing 1 million m^3 of fresh water per day it requires annually about 8.8 million tons of oil [4, 5]; therefore, using renewable energy resources are essential.

Parabolic trough collectors (PTC) are the most matured and commonly used among solar concentrators simply because of their efficiency, less equipment requirement for control (single axis), utilization of land, modularity and actual field implementation. Also, when using PTC for desalination purposes they are more economical and cost effective [6]. PTC can supply direct solar thermal energy to produce fresh water in desalination plants that uses evaporation techniques. However, since solar energy is time variant in both daily and monthly as well as weather-affected, fuel may be used to augment the deficiency in solar energy in order for the system to remain economically feasible [7, 8]. For example, for localities with latitudes above the equator during the month of January the solar altitude angle is considerably lower than what it is during the summer months which influence the PTC performance. The benefits of employing and utilization of renewable energy resources for desalination purposes in addition to lowering cost, will eventually lead to reduction in the amounts of carbon dioxide in the atmosphere and thus their levels remain under control to an acceptable values.

Recognizing the significant amount of energy requirement for this technology a comparison among the various methods available for desalination was made [4] and it was shown that reverse osmosis (RO) is the least for consuming energy but has high equipment cost. For reverse osmosis with energy recovery the benefits of reducing required energy is even more but the system is only cost effective at large scale operations. The method known as multiple effect desalination (MED) is next to (RO) in terms of energy requirements where it is estimated that it consumes about 150 kJ/kg of freshwater product which is about the same for RO when considering the electric energy. Multi-Stage flash (MSF) is more energy demanding than RO or MED where it is estimated that it requires about 340 kJ/kg of product but it is comparable to MED in terms of equipment cost. However, according to [3] MSF are more common worldwide where they have about 26% of the market share versus about 8% for MED. Also, for the MED and MSF they are more attractive especially in areas of high polluted water since they involve water boiling which have the benefits of reducing pathogens and microbes if not eliminating their infiltration into the fresh water. Other researchers have investigated the various concentrators effects on the desalination efficiency [9]. Other desalination concepts included evaluating organic-fluid Rankine cycle driven by a PTC collector where the electricity generated is used to drive pumps for reverse-osmosis desalination [10, 11, 12, 13]. Such schemes are most likely will entail more capital and maintenance costs as well as being perhaps undesirable in areas with polluted waters.

Significant research activities using PTC for desalination were conducted at the Plataforma Solar de Almer´ıa (PSA) which started in the nineties and showed the technology is feasible; however the cost of production was still high and not competitive with conventional means. The PTC used synthetic oil to transfer solar heat to heat up seawater. Other ideas of improving the system performance has lead to another project known as AQUASOL; specifically, ideas as employing double-effect absorption heat pump at the end of the MED and lowering the electrical demands by the use of steam ejectors as well as using compound parabolic concentrator as an alternative to PTCs [14].

However, upon reviewing the literature no one has seemed to address the effects of tilting the PTC in the case of desalination application for the purpose of increasing the utilization of solar energy thus improving the annual production rate of fresh water which would consequently lead to lowering cost. Tilting the PTC at small angles will unlikely cause significant structural problems; however, the gain in performance, as quantified here, is of significance.

Although the use of PTC for seawater desalination has not been commercialized; however the PTC technology is a matured one and has been commercially demonstrated in power generation as for example in the SEGS, Mojave Solar Project, Solana Generating Station and Genesis solar Energy which all currently operated in the USA with SEGS is the longest in operation since 1984 [15]. Perhaps for PTC seawater desalination the initial capital cost leads to higher levelized cost that is not acceptable to the masses; therefore, by combining several methods that are intended to improve the gained output ratio (GOR) will pave the way for commercializing the use of PTC in desalination. Methods of improvements can include the tilt angle which is the subject herein along with others like use of thermal vapor compression (TVC) and use of absorption cycles. A current study is being conducted to address such issue and their final impact on the levelized cost.

The work herein intends to quantify the improvement achieved by slightly tilting the PTCs for specific months with the tilt made once per month. The study was motivated by an earlier investigation [17] which considered the optimization of the annual fresh water production from a similar scheme using pure water properties rather than seawater's while maintaining the PTC at zero tilt angle. However, the current investigation as before considers the same scheme which includes a PTC assembly, fuel-fired boiler and Multi-Stage Flash chambers (MSF) with the PTC allowed to be tilted at low angles once per month. Also, actual seawater properties were used in the simulation. The seawater is directly heated in the PTC thus eliminating any associated cost with thermal oil as a heating transfer fluid. Heating seawater directly in the PTC is made possible since the seawater is forced to remain in liquid and exiting PTC as saturated liquid which gave good heat transfer coefficient as was suggested in [17]. Also for seawater to remain in liquid forms adds the benefits that it reduces the potential of scaling. For performance evaluation, a minimum on the rate of fresh water generation is set whereby if solar radiation is not enough fuel heat augments the deficiency so that the minimum rate is achieved. The scheme generates as much of fresh water when solar is abundant. Thus, the scheme does not include any thermal storage methods which would entail complexity and more cost. The rational for not having thermal storage when solar is abundant is that produced fresh water is stored more conveniently than thermal energy. Additionally, the study showed that the operating pressure affects the water production rate, although to a lesser degree, whereby rates are seen to approach maximum when operating pressure is above 20 bar for the water as it passes the absorber tube. However, increasing the saturation temperature beyond 120 °C would increase scaling problems, thus in this study the seawater pressure while in PTC was set at 2.0 bar; corresponding to saturation temperature ~120 °C. The effect of tilt angle of the PTC were examined at 0°, 10°, and 20°. The tilting of the PTC is assumed to be performed once a month which is unlike the instantly daily single axis control for tracking the sun. Therefore, PTC tilting would not be expected to incur additional operational cost; however, initial capital cost would be more as a result of the extra structural strength required for supporting tilting as well as the required mechanisms.

2.0 SCHEME AND MODELING

Figure 1 shows the solar-fuel scheme for desalinating seawater whereby fuel heat is added to maintain a preset daily minimum fresh water production at times of low solar irradiation. Seawater is pumped to the system operating pressure using a feed water pump and simultaneously is preheated while it is used to condense vapor generated in the consecutive Multi-Stage Chambers (MSF). After coming out of the MSF, the seawater splits with one stream going to the PTC with a flow rate to allow it to reach saturated liquid as it leaves the absorber and the other stream is directed through the fuel-fired boiler, where fuel heat is added just to bring seawater to liquid saturation. However, when the flow rate through the PTC exceeds the preset daily minimum, as a result of solar abundance, then no flow rate through the fuel-fired boiler is required and in this case it is set to zero. The flow rate of seawater through the PTC varies during the day because of the variation in solar irradiation. The combined heated seawater from the PTC and the boiler is allowed to flash in the MSF chambers which have a decreasing flashing temperatures until reaching the last one where it is set 10 °C higher than the prevailing seawater temperature for that month (Table 1). The seawater pressure in the PTC was set at 2 bar (~120 °C saturation temperature). The delta decrease in the flashing temperatures in the MSF was set in the range (5-6) °C for the consecutive chambers; thus same number of chambers (16) was always used. Each chamber was assumed to have 85% effectiveness for condensing vapor. The inlet seawater was set at the temperatures given in Table 1 for the corresponding months.

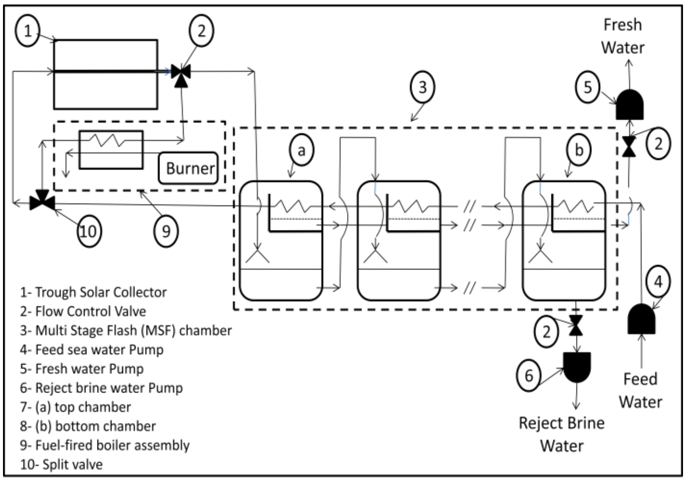

Figure 1. Solar-fuel desalination scheme.

For modeling, the approach was to use a PTC that has characteristics based on the SEGS program which is oriented north-south, has an aperture area 70.4 m^2 for capturing the solar radiation and directing it at the absorber. Further description of the selected PTC and approach are given in [17]. The PTC, with a tilt angle β from the horizon, is allowed to track the sun per the computed solar altitude α and azimuth ϕ angles. In order to determine the incident angle α' on the plane of PTC and its rotation angle ϕ_{PTC} the following unit vectors were derived: a) a normal to plane of PTC, equation (1); b) the projection of the normal to PTC aperture on the *xy* plane, equation (2); and c) a vector along the incident beam, equation (3); see Figure 2.

$$\hat{r}_{PTC} = \cos(\alpha)\sin(\varphi)\hat{i} + \sin(\alpha)\cos(\beta)\hat{j} + \sin(\beta)\hat{k} \tag{1}$$

$$\hat{r}_{PTC,n} = \cos(\beta)\hat{j} + \sin(\beta)\hat{k} \tag{2}$$

$$\hat{r}_{I} = \cos(\alpha)\sin(\varphi)\hat{i} + \sin(\alpha)\hat{j} + \cos(\alpha)\cos(\varphi)\hat{k} \tag{3}$$

Consequently, the rotation and the incident angles for the PTC are

$$\cos(\varphi_{PTC}) = \frac{\hat{r}_{PTC} \cdot \hat{r}_{PTC,n}}{\left\|\hat{r}_{PTC}\right\| \times \left\|\hat{r}_{PTC,n}\right\|}, \quad \cos(\alpha') = \frac{\hat{r}_{PTC} \cdot \hat{r}_{I}}{\left\|\hat{r}_{PTC}\right\| \times \left\|\hat{r}_{I}\right\|} \tag{4}$$

The direct beam intensity I_n and solar angles; i.e., incident and azimuthal, were computed based on the outlined procedure given in [18, 19] and was used for solar prediction in [16, 17, 20].

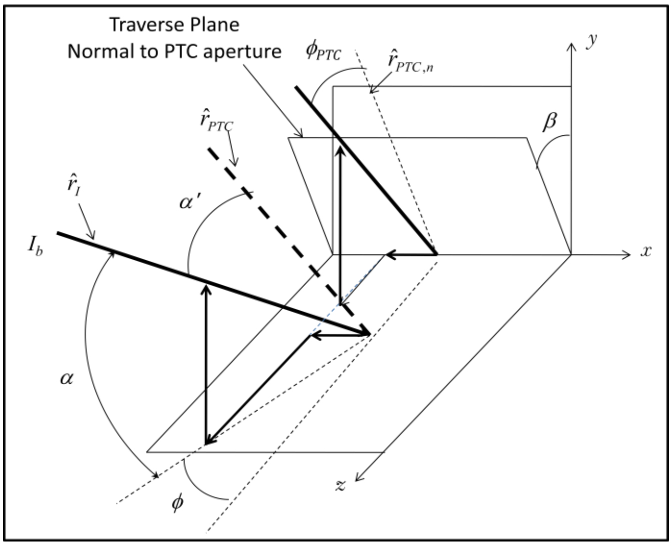

Figure 2. Definitions of incidence, tilt, rotation angles and unit vectors.

For the absorber tube the governing equations are deduced from the energy and mass conservations which are written for a segment of the tube, Figure 3. Considering fixed control volume, the governing equations for the absorber tube which include the fluid flow, the steel tube and the encasing glass tube are [17],

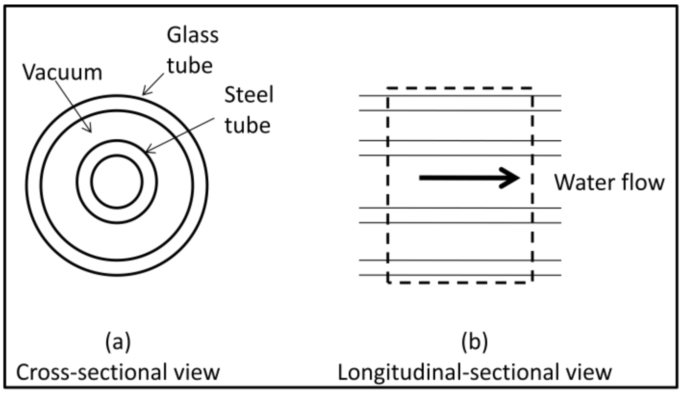

Figure 3. Finite control volume used for the development of the governing equations.

$$\delta V_w \frac{\partial \rho u}{\partial t} + \dot{m}_w \Delta h = h_w \delta A_{si}\left(T_s - T_w\right) \tag{5}$$

$$\begin{aligned}\delta m_s c_s \frac{\partial T_s}{\partial t} &= \gamma\rho\tau\alpha\delta A_{ap} I_n \cos(\phi) K(\phi) \\ &\quad - h_w \delta A_{si}\left(T_s - T_w\right) - \left[-k_s \delta A_{sc} \frac{\partial^2 T_s}{\partial z^2}\right]\Delta z \\ &\quad - \varepsilon_s \sigma \delta A_{so}(T_s^4 - T_g^{4)}) - \varepsilon_{slw}\delta A_{so}\sigma\left(T_s^4 - T_{sur}^4\right)\end{aligned} \tag{6}$$

$$\begin{aligned}\delta m_g c_g \frac{\partial T_g}{\partial t} &= \gamma\rho(1-\tau)\delta A_{ap} I_n \cos(\alpha) K(\phi) + \varepsilon_g \delta A_{so}\sigma\left(T_s^4 - T_g^4\right) \\ &\quad - \varepsilon_g \delta A_{go}\sigma\left(T_g^4 - T_{sur}^4\right) \\ &\quad - \delta A_{go} h_\infty\left(T_g - T_\infty\right) - \left[-k_g \delta A_{gc}\frac{\partial^2 T_g}{\partial z^2}\right]\Delta z\end{aligned} \tag{7}$$

$$u = u(P,x), \quad h = h(P,x); \text{when fluid exists as two phase} \tag{8}$$

$$u = u(P,T), \quad h = h(P,T); \text{when fluid exists as liquid only} \tag{9}$$

The internal energy, enthalpy, temperatures, heat transfer coefficients are both time and spatial-dependent (in the z-direction: along tube) since the flow conditions are changing which is consequent to the variation in the daily solar irradiation. The equations were discretized and solved using finite difference methods. During the solution, the mass flow rate of the seawater through the absorber tube was adjusted as a consequence to the changes in the solar irradiation so that to result in the seawater at the exit of it as saturated liquid. The flow conditions inside the tube varies with the fluid flow rate (laminar/turbulent), fluid temperature, tube temperature and solar intensity and consequently affect Nusselt number which in turn influence the heat gained by the fluid. Therefore, an iterative approach was employed to obtain the solution at each time increments to determine the correct mass flow rate for the given instant time during the day and consequently the amount of fresh water is determined. The determination of the fresh water in the MSF is based on thermodynamic and heat transfer principles. Specifically, from the determined hot mass flow rate of seawater coming from the PTC/boiler and the vapor quality in each chamber (as a result of the flashing) the rate of vapor flow is calculated which in turn preheats the induced cold seawater at an assumed effectiveness 85%. The preheating comes from both latent and sensible heat of the vapor. Further details of the solution are given in [17]. The thermophysical properties of seawater were obtained using resources available in [21].

The solutions were obtained at tilt angles 0°, 10° and 20° for the months and the conditions as given in Table 1. In the table, the ambient temperatures are taken from [22] which are representative of the locality considered for the analysis while the seawater temperatures are taken from [23].

Table 1. Months used in analysis with ambient temperatures and tilt angles.

Month	January	March	June	August	October	December
Mean T_∞, °C*	8.0	11.75	23.6	25.35	20.35	9.75
Sea T	15	17	28	25	20	15
Tilt angles	0°, 10°, 20°	0°, 10°, 20°	0°	0°	0°, 10°, 20°	0°, 10°, 20°

- Data from [22, 23].

3.0 Model Verification

The verification of the modeling was made at three levels. For level one, the input solar parameters which include beam intensity and solar angles were computed using a model that was developed earlier and repeatedly validated previously. However, validation also was made for the current study by comparing the total daily direct solar against experimental data obtained by [24] at location 32:05' N and 36:07 E. The measured value of the total daily of direct solar was found to be 26.0 MJ/m^2 for a horizontal surface on June 15 which compares well with the value 26.7 MJ/m^2 computed from the predictive model. The experimental data was reported to have +/-5% accuracy and accounted for irradiation between the hours 8:00 AM to 3:00 PM. However, the results to follow (Section 4) solar irradiation is considered for the entire light-day period. Except for the months of January and December, the validation of the rest of the considered months are shown in Table 2. As it appears from the table the predicted solar input parameters are within 5.7% for the hot months (June and August) and up to 26% higher for the cold months (March and October). The reason for the large discrepancy for the cold months is the overhead clouds which obscures direct beam. For the months of January and December they were not included since they are known, for the region of study, to be mainly heavily clouded which was not accounted for in the predictive model.

Table 2. Comparison of calculated total daily beam with experimental data. Data are taken on the 15th day.

Month	March	June	August	October
Calculated, MJ/m^2	21.9	26.7	24.3	17.7
Experimental*, MJ/m^2	19.0	26.0	23.0	14.0
Percent error	15.3	2.7	5.7	26.4

The second level of validation was concerning the numerical solution by considering consistency and convergence whereby smaller spatial and time steps were assessed. The spatial increment 0.2 m was observed to yield consistent solutions when compared with smaller spatial steps. The time step was set 10 seconds maximum and consequently was reduced so that no temperature greater than 0.5 °C results during the solution. The time step is considerably less than what the criterion of the method calls for which resulted in stable solutions.

Thirdly, the model was used to compute the operational thermal efficiency of the PTC under the operational conditions for the month of June and it was compared against published data with similar conditions. Here, the term operational efficiency is used to distinguish it from typical efficiency which is normally measured under lab conditions with normal beam incidence. Variation of operational efficiency from month to month is expected as a result of variation in solar angles and ambient conditions. Figure 4 shows the computed June operational efficiency using water with salinity 36 g/kg versus the reduced temperature and it is compared against experimental data from two sources. For the experimental data from [25] it was taken during October time at locality 52.6 E and 29.6 N for a PTC with 25 m long, 3.4 m wide and using oil as heating transfer fluid. The optical properties reported of the PTC were better than what used in the analysis. Evidently the agreement between the prediction and this set of data is within 6%. The other comparison is made against data collected from SEGS/Kramer Junction, California during June/1998 using synthetic oil. For lack of inlet temperature of the oil going to the PTC, the reduced temperature could not be calculated; however, the efficiency between the hours 9:00 AM – 4:00 PM was observed to be in the range (61% – 64%). For this reason, the data are shown at the right of the figure. Again the model prediction in general falls within the experimental data. To emphasis the last comparison is a general one and gives indication to the truthfulness of the results.

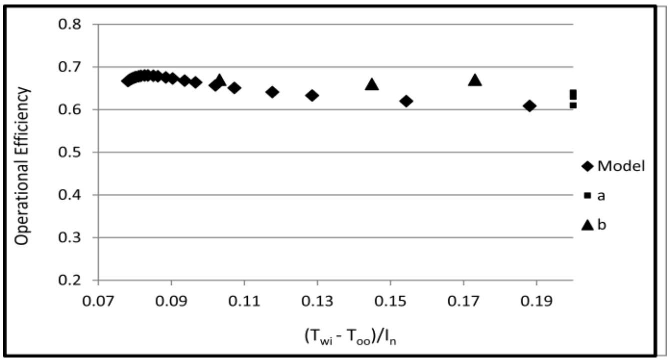

Figure 4. Comparison between computed operational efficiency against experimental data. a source [25.

4.0 RESULTS

Figure 5 shows the hourly induced seawater through the PTC while being heated by it and leaving the absorber tube as saturated liquid under solar conditions for the months of January with zero and 20° tilt angles and for the month of

June with zero tilt. Evidently, the highest flow rates of seawater through the PTC are realized during the month of June which is a consequent to the high solar irradiation as well as to longer light hours. Note that in the modeling scheme the flow rate through the PTC changes during the day following the hourly irradiation variation so that the seawater exits as saturated liquid. Also certain flow rate of seawater is necessary to assure generating a minimum hourly fresh water rate which was arbitrarily set 0.2 kg/s. To obtain this fresh water rate the minimum required seawater flow rate in the scheme was found 1.444 kg/s, hence if the seawater flow rate through the PTC drops below this value the fuel-fired boiler augments the difference in required heat. The improvement of PTC performance for the month of January with tilt angle is clearly demonstrated in the figure by accepting more seawater flowing through it which is seen to reach 1.2 kg/s around noon time; but, not enough to meet the minimum flow rate of seawater 1.444 kg/s; thus fuel heat would be required during the entire days of this month.

The hourly rate of gained solar energy along with the required fuel heat are shown for the months of January and June in Figures 6 and 7; respectively. Figure 6 shows that for the month of January during the mid day hours the gained-solar energy averages about 28 kW while the required fuel heat is about 15 kW when the PTC tilt angle is zero. However, the effect of the tilt angle is seen during mid-day hours that for 20° where the gain in solar is increased by about 29% and simultaneously reducing the required fuel heat about 60%. Note for the month of June (Figure 7) no fuel is required for most of the day to deliver the desired fresh water or more; thus leaving the cost of fresh water production only due to pumping power. Also note the fuel heat requirement calculations are made during the day light thus the length of operational hours changes from month to month.

The total daily production of fresh water by during several months at various tilt angles is depicted in Figure 8. Recall that the minimum production rate was arbitrarily set to 0.2 kg/s for fuel augmentation. The figure reveals the amount of fresh water produced by solar energy and that due to fuel heat. For the month of January even with a 20° tilt the required fuel heat to the total daily production is about 40% and slightly worse for the month of December. However, for the month of March the contribution of fuel heat was reduced from about 19% for zero tilt to 8% for 20° tilt which brings it better than the month of August which has fuel heat contribution of 16% of the total required energy; the month of June is exceptionally well where the fuel heat contribution is about 8% of the total consumed energy with zero tilt angle. It is evident from the figure that for this scheme with one PTC when tilt angle is included, fresh water is generated from solar alone for most of the year (month of March through October) at a daily rate of about 6.5 m^3 to 8.2 m^3; or in terms of surface area corresponding to 0.0923 m^3/m^2 to 0.116 m^3/m^2; respectively, compared to 0.034 m^3/m^2.

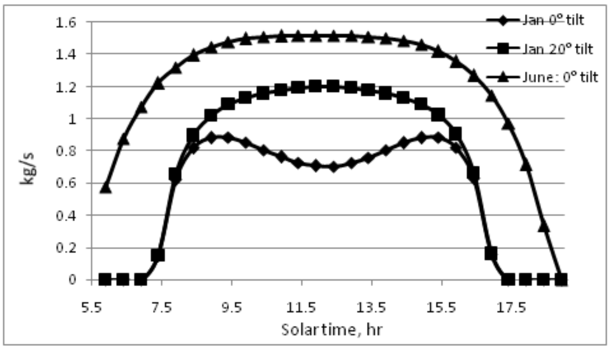

Figure 5. Hourly rate of seawater flowing through the PTC.

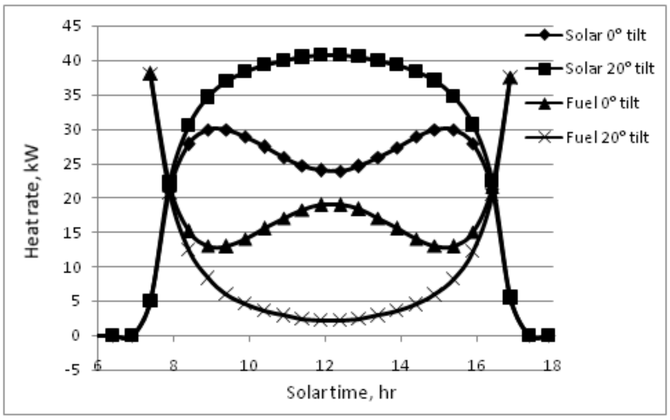

Figure 6. Hourly rate of gained solar energy and fuel heat added to maintain a minimum of fresh water production 0.2 kg/s. Month of January with PTC at 0° and 20° tilt angle.

For producing the amount of fresh water shown in Figure 8, the required daily energy by solar, fuel and electricity is given in Figure 9. The electric pumping is required to force the seawater through the PTC which is maintained at 2.0 bar as well as to pump the fresh and reject water from the low pressure of the last chamber of MSF to atmospheric pressure. For the month of June it is seen that 290.8 MJ and 73.7 MJ of energy in the form of heat and electricity; respectively, are required to supplement the generation of about 9.0 m^3/day of fresh water; with the assumption 85% pump efficiency for computing the electric energy. Assuming a conversion efficiency of 30% for electricity, 80% for the fuel boiler, calorific value for the fuel of 45 MJ/kg and 0.85 specific gravity, then this means that about 1.75 liter of fuel is required for generating 1 m^3 of fresh water in the month of June. At present fuel prices this could be challenging for some countries; therefore, the cost could be brought further down by lowering the minimum desired rate of fresh water production which entails increasing PTC modules. Additionally, observe that for the month of March with 20° tilt comparable results are obtained as for the month of August which indicates the importance of the tilt angle for producing nearly uniform rate for most of the year; i.e., for the months of March through October.

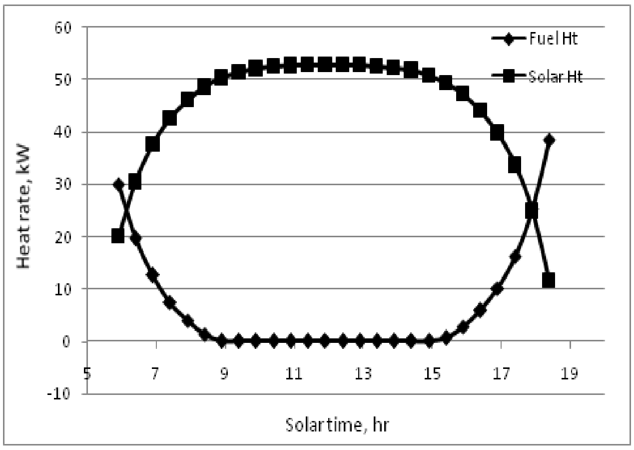

Figure 7. Hourly rate of gained solar energy and fuel heat added to maintain a minimum of fresh water production 0.2 kg/s. Month of June with PTC at 0 tilt angle.

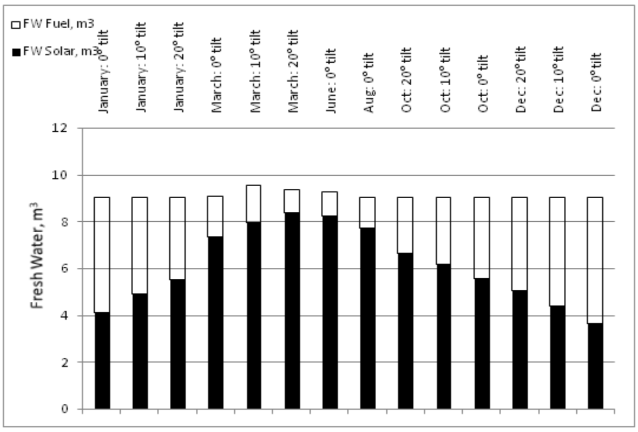

Figure 8. Solar and fuel contribution to the total daily production in various months at different tilt angles.

Alternatively, the importance of the tilt angle on the system performance is demonstrated in Figures 10 which shows the hourly rate production of fresh water for the month of March at tilt angles 0°, 10° and 20°. Clearly the rate of production is enhanced with the tilt angle because the incident angle is reduced with the increase in the tilt angle which leads to improving both the amount of absorbed radiation and the optical properties; the optical properties are modeled using the incidence modifier as explained in [17]. The preceding improvement is evident in the enhanced annual efficiency of the PTC, calculated as solar gained by seawater to total incident irradiation, Figure 11; where for the months of June and August were made only for zero tilt angle thus the lines for 10° and 20° tilt angles appear disconnected. The daily efficiency for the month of March improved from 57.5% at 0° tilt, to 62.1% at 10° tilt and to 65.4% at 20° tilt.

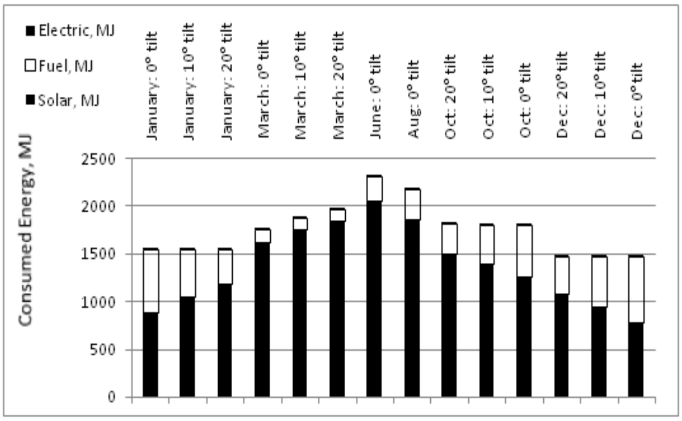

Figure 9. Daily consumed total solar, fuel and electric energy for the production of fresh water (given in Figure 8).

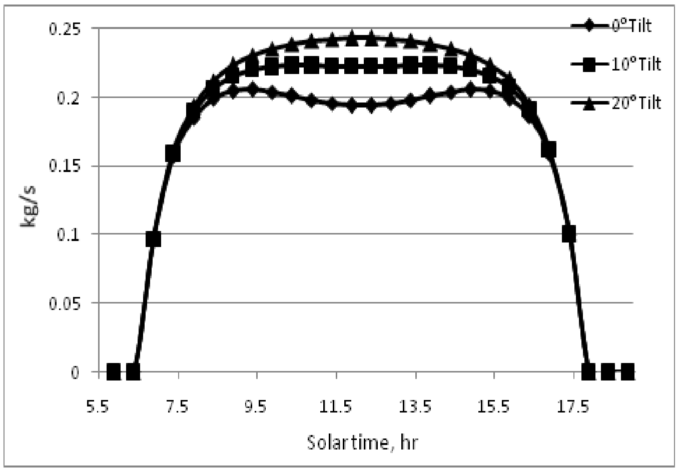

Figure 10. Hourly rate of fresh water production for the month of March at 0°, 10°, 20° tilt angles.

Figure 12 shows the annual performance ratio (PR) variation with tilt angles per each month. The performance ratio is defined as the kilogram of fresh water generated divided by units of consumed energy converted to kilogram of steam (2300 kJ per kg of steam). The consumed energy includes the gained solar, the heat from fuel and the electrical due to pumping. No conversion of electrical to fossil fuel was used. Strikingly, the month of June yields the lowest PR, slightly above 9. Also, clearly shown that the tilt angle has no effect on the PR for any specific month when the tilt angle changes since the increase in the amount of fresh water results from the better utilization of the solar energy. The main reason for the low PR in the hot months and high PR for the cold months is mainly due to hot and low seawater temperatures for these months; respectively (Table 1). The effects of low temperature for the incoming seawater to the MSF was recognized by other researchers.

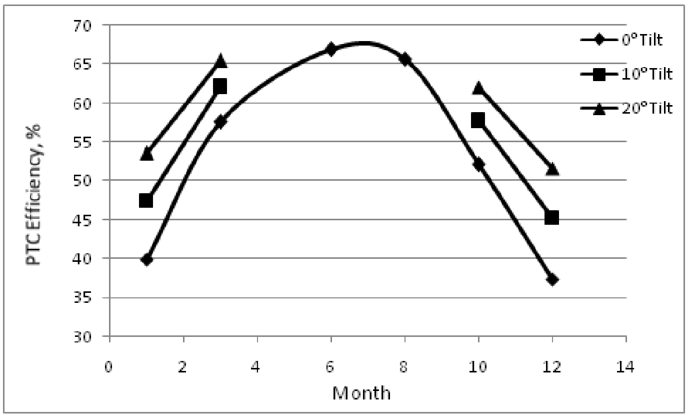

Figure 11. Daily efficiency of the PTC during the year at 0°, 10°, 20°.

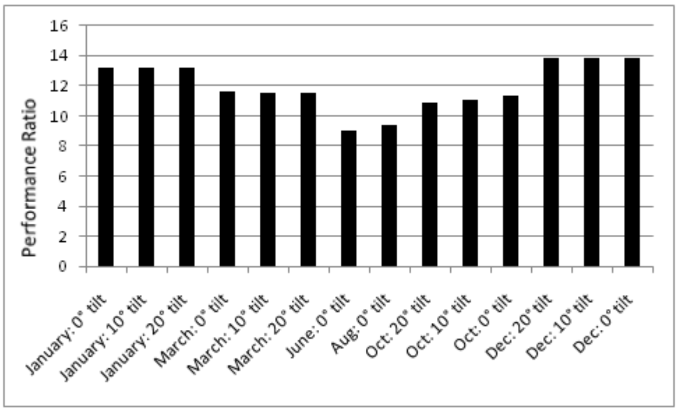

Figure 12. Performance ratio variation over the entire year.

CONCLUSIONS

A solar-assisted seawater desalination scheme using parabolic trough collector with fuel augmentation was considered for analytical evaluation for the annual production of fresh water. The results of the analysis were confirmed experimentally and analytically. Fuel heat is only added when the production of fresh water falls below a pre-set desired level (0.2 kg/s); however, the scheme produces more than the desired rate during high solar irradiation. The characteristics of the PTC used in the analysis is based on those used in the SEGS LS-2 program that has an aperture area 70.4 m^2. The results shown herein are based on one PTC module. The effect of tilt angle of the PTC was evident for the months with low altitude angles; however, for the months with high altitude angles the effect of tilt angle was less. For months with low solar altitude angles it was revealed that with a tilt angle of 20° it resulted in increasing the fresh water production due to only solar for the months of March and October by 14% and 19%; respectively, corresponding to daily total production of 8.4 m^3 and 6.6 m^3 compared to 8.3 m^3 for June with no tilt. Equivalently, the reduction in fuel at 20° was observed to be 15% and 44%; respectively for the months of March and October compared to no tilt. This brings the importance of tilt angle on increasing the utilization of solar energy and reducing the fuel heat required for producing fresh water. To summarize the tilt angle permits the scheme to produce from 8.4 m^3 to 6.6 m^3 for most of the year (from month of March through October). It is important to emphasis that the amount of consumed fuel depends on the arbitrarily pre-set minimum production rate of fresh water which explains that the enhanced in water production did not linearly correspond to the fuel reduction.

REFERENCES

[1] Li C., Goswami Y., Stefanakos. Solar Assisted Sea Water Desalination: A review. Renewable and Sustainable Energy Reviews, 2013 Vol 19, 136-163.

[2] United Nations (Ed.), Water for People, Water for Life — UN World Water Development Report, UNESCO Pub., New York, 2003.

[3] The IDA Desalination Yearbook 2011–2012, Water desalination report.

[4] Kalogirou, S, Use of Parabolic Trough Solar Energy Collectors for Seawater Desalination. Applied Energy, 1998, Vol. 60: 65-88.

[5] Kalogirou SA. Seawater desalination using renewable energy sources. Progress in Energy and Combustion Science 2005;Vol 31:242–81.

[6] V.K. Jebasingh, G.M. Joselin Herbert. A review of solar parabolic trough collector. Renewable and Sustainable Energy Reviews, 2016, Vol 541085–1091.

[7] El-Nashar AM. The economic feasibility of small solar MED seawater desalination plants for remote arid areas. Desalination 2001;Vol 134:173–86.

[8] El-Nashar AM. Economics of small solar-assisted multiple-effect stack distillation plants. Desalination 2000;Vol 130:201–15.

[9] Saettone, E., Valencia. Comparison between Solar Distillers with and without Solar Concentrator. J Applied Solar Energy, 2016, Vol 52, pp 131–136.

[10] Bruno Joan Carles, Lopez-Villada Jesus, Letelier Eduardo, Romera Silvia, Coronas Alberto. Modelling and optimization of solar organic rankine cycle engines for reverse osmosis desalination. Appl Therm Eng2008;Vol 28:2212–26.

[11] NafeyAS, Sharaf M A.Combined solar organic Rankine cycle with reverse osmosis desalination process: energy, exergy, and cost evaluations. Renew Energy 2010;Vol 35:2571–80.

[12] Sotirios, K., Konstantinos, T., Dimitrios, M., Investigation of an autonomous hybrid solar thermal ORCePV RO desalination system. The Chalki island case. Renew Energy 2011; Vol 36:583–90.

[13] Sharaf MA, Nafey AS, Garcia-Rodriguez Lourdes. Exergy and thermo-economic analyses of a combined solar organic cycle with multi-effect distillation desalination process. Desalination 2011; Vol 272:135–47.

[14] Alarco´n-Padilla D-C,Garcı´a-Rodrı´guez L.Application of absorption heat pumps to multi-effect distillation: a case study of solar desalination. Desalination 2007;Vol 212:294–302.

[15] USA Energy Information Administration Website: https://www.eia.gov/energyexplained.

[16] AK Ababneh 'Assessment of Annual Yield of Fresh Water from A Hybrid Desalination Scheme Utilizing Solar Parabolic Trough', International Journal of Environmental Science, 2016, Vol 1:151-55.

[17] A.K. Ababneh, A. Jawarneh, H. Tlilan, N. Duic, 'Performance Evaluation of Solar Parabolic Trough Collector for the Application of Sea Water Desalination', IREME, 2016, Vol 10: 443- 51.

[18] ASHREA Handbook, Fundamentals, 1993.

[19] Energy Conversion, D. Y. Goswami, F. Kreith, Taylor and Francis Group, 2007.

[20] A. Ababneh 'Energy Conservation Using a Double-effect Absorption Cycle Driven by Solar Energy and Fossil Fuel', JJMIE, , 2011, Vol 5, No 3, pp 213-219.

[21] MH Sharqawy, JH Lienhard V, SM Zubair, 'Thermophysical properties of seawater: A review of existing correlations and data', Desalination and Water Treatment, 2010, 16, 354-380.

[22] Heating and Air Conditioning, M. A. Alsaad, M. A. Hammad, 3rd edition.

[23] VC John, SL Coles, A Abozed 'Seasonal cycles of temperature, salinity and water masses of the Western Ara bian Gulf', *Oceanologica Act*, 1990, 13, 3, 273-281.

[24] AM Jawarneh, M Al-Tarawneh, A Ababneh, H Tlilan, 'Solar Energy Availability on Horizontal and Tilted Surfaces: a Case Study', IREME, Vol 6, N4, May 2012.

[25] A. Mokhtari[a], M. Yaghoubi[a]*, P. Kanan[b], A. Vadiee[a]. R. Hessami[a] 'Thermal and optical study of parabolic trough collectors of Shiraz solar power plant', Proceedings of the Third International Conference on Thermal Engineering: Theory and Application, Amman-Jordan, May 2007.